Skeletal development in sloths and the evolution of mammalian vertebral patterning

Lionel Hautier[a,1], Vera Weisbecker[b], Marcelo R. Sánchez-Villagra[c], Anjali Goswami[d], and Robert J. Asher[a,1]

[a]Department of Zoology, University of Cambridge, Cambridge CB2 3EJ, United Kingdom; [b]Department of Earth Sciences, University of Cambridge, Cambridge CB2 3EQ, United Kingdom; [c]Paläontologisches Institut und Museum, Universität Zürich, 8006 Zürich, Switzerland; and [d]Department of Genetics, Evolution, and Environment and Department of Earth Sciences, University College London, London NW1 2HE, United Kingdom

Edited by Clifford J. Tabin, Harvard Medical School, Boston, MA, and approved September 24, 2010 (received for review July 16, 2010)

Mammals show a very low level of variation in vertebral count, particularly in the neck. Phenotypes exhibited at various stages during the development of the axial skeleton may play a key role in testing mechanisms recently proposed to explain this conservatism. Here, we provide osteogenetic data that identify developmental criteria with which to recognize cervical vs. noncervical vertebrae in mammals. Except for sloths, all mammals show the late ossification of the caudal-most centra in the neck after other centra and neural arches. In sloths with 8–10 ribless neck vertebrae, the caudal-most neck centra ossify early, matching the pattern observed in cranial thoracic vertebrae of other mammals. Accordingly, we interpret the ribless neck vertebrae of three-toed sloths caudal to V7 as thoracic based on our developmental criterion. Applied to the unusual vertebral phenotype of long-necked sloths, these data support the interpretation that elements of the axial skeleton with origins from distinct mesodermal tissues have repatterned over the course of evolution.

constraint | heterochrony | vertebrae | ontogeny | Xenarthra

Conservatism in the mammalian axial skeleton, including that exhibited by nonmammalian synapsids, is substantial (1). All but a few of ~5,000 living mammal species possess exactly seven neck vertebrae; other presacral counts also show lower interspecific variation in mammals than in nonmammals (2–5). Only three genera show departures from the cervical constant: manatees (*Trichechus*) and tree sloths (*Choloepus* and *Bradypus*). Recent progress in understanding the mammalian component of the tree of life places these departures among afrotherians and xenarthrans, two groups that are likely sister taxa (6, 7). These exceptions to the rule of seven have intrigued the anatomists since the 18th century. For example, in 1765, the Comte de Buffon (8) noted the different number of neck and rib-bearing vertebrae in *Choloepus* and *Bradypus* and considered them as "une erreur de la nature; car de tous les animaux . . . aucun n'a tant de chevrons à la charpente" (a "mistake of nature, because among all animals . . . none has so many bones in its belfry") (8).

The genetic basis of axial skeleton patterning across vertebrates is relatively well-documented (9, 10), and stabilizing selection may play an important role in the conservatism observed in many of these species (11). Another explanation for departures from a conserved vertebral count, one that does not exclude a role for stabilizing selection, involves a level of independence of regions of the axial skeleton derived from somitic vs. lateral plate mesoderm. With the caveat that some somitic precursor cells migrate into the lateral plate early in development, these tissue domains have been dubbed primaxial (vertebrae and proximal ribs) and abaxial (limb girdles), respectively (12). Buchholtz and Stepien (13) have proposed a primaxial–abaxial shift (PAS) to explain aberrant vertebral counts of sloths (Xenarthra and Pilosa). They observed that, in cases of intraspecific variation, primaxial skeletal elements appear to be shifted relative to abaxial elements in sloths with atypical cervical vertebral counts.

Here, we present developmental data for mammals that bear directly on the claim that a primaxial–abaxial shift has taken place in sloths. We propose criteria based on ossification sequences to distinguish between cervical and thoracic vertebrae. Neck vertebrae (i.e., those without ribs located cranial to the shoulder girdle) are typically synonymous with cervical vertebrae among mammals. We argue that this is not the case in sloths, species of which may show ribless thoracics in the neck or ribbed cervicals in the thorax. We find that ossification sequences characteristic of true cervical vertebrae are conserved across mammals, including in the sloth neck, despite their morphological divergence. Thus, even the few mammals that deviate from the rule of seven do so by maintaining the identity of what remain cervical and thoracic vertebrae based on developmental criteria.

Results

Ossification of the Vertebral Column in Mammals. All mammals in our dataset, except for sloths, show a highly consistent ossification pattern of centra relative to neural arches and of cervical centra relative to those located more distally. Specifically, the neural arches begin ossification in the neck region, before or coincident with the neural arches of the cranial thoracic region (Datasets S1, S2, S3, and S4). In addition, neural arches ossify faster than centra throughout the spine. The first appearance of centra occurs after the ossification of the neural arches of the cranial-most rib-bearing vertebra. Centra ossify first among the rib-bearing and lumbar series, adjacent or caudal to the developing clavicles and scapula, followed by the spread of ossification in both a cranial and caudal direction. Most consistently, we observed late ossification of caudal cervical centra relative to those of the rib-bearing region in all mammals in this dataset except three-toed sloths, and in most mammals, caudal cervical centra ossified after those in the lumbar region as well. Only in the marsupials *Sminthopsis macroura* (14), *Isoodon macrourus*, and *Macropus eugenii* did cervical centra ossify before lumbar ones but never before thoracic centra. Among all nonsloths for which we have data (Datasets S1, S2, S3, and S4), including monotremes, marsupials, and placentals, the centra never precede ossification of neural arches in the neck.

Skeletogenesis in Armadillos. For comparison with other xenarthran mammals, we present data on vertebral ossification in a cingulate xenarthran, *Dasypus* (long-nosed armadillos) (Dataset S3). The neural arches of the atlas and axis are the first vertebral elements to ossify in *Dasypus*. Ossification then appears in the cranial thoracic region (Fig. 1*A*) and is quickly followed by the upper neck and upper lumbar regions (Fig. 1*B*). Ossification

Author contributions: L.H. and R.J.A. designed research; L.H., V.W., M.R.S.-V., A.G., and R.J.A. performed research; L.H., V.W., M.R.S.-V., A.G., and R.J.A. contributed new reagents/analytic tools; L.H., V.W., M.R.S.-V., A.G., and R.J.A. analyzed data; and L.H. and R.J.A. wrote the paper.

The authors declare no conflict of interest.

This article is a PNAS Direct Submission.

[1]To whom correspondence may be addressed. E-mail: ljh75@cam.ac.uk or r.asher@zoo.cam.ac.uk.

This article contains supporting information online at www.pnas.org/lookup/suppl/doi:10.1073/pnas.1010335107/-/DCSupplemental.

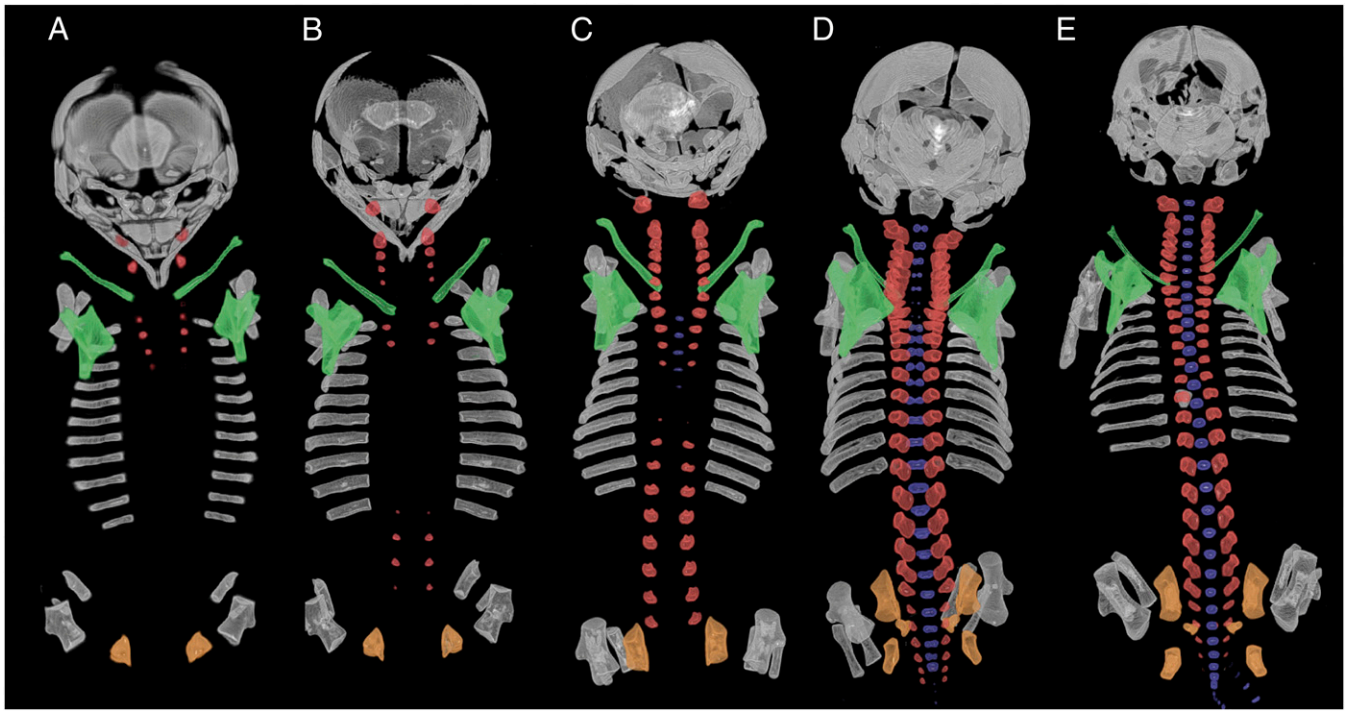

Fig. 1. Dorsal view of the skeleton in armadillos: (*A*) *Dasypus kappleri* (ZMB k28) crown rump length (CRL) = 43 mm. (*B*) *Dasypus novemcinctus* (ZMB 85893) CRL = 43 mm. (*C*) *Dasypus sp.* (ZMB 6532) CRL = 46.5 mm. (*D*) *Dasypus sp.* (ZMB 12XII01) CRL = 50 mm. (*E*) *Dasypus novemcinctus* (ZMB 7b) CRL = 68 mm. Vertebral neural arches are in red, vertebral centra are in blue, scapula and clavicle are in green, and ischium, ilium, and pubis are in orange. For clarity, elements of the autopod have been removed.

spreads cranially from the upper lumbar region and caudally from the upper thoracic region to meet at the middle of the rib cage (Fig. 1*C*). The sacral and caudal neural arches are the last to ossify (Fig. 1 *D* and *E*). Ossification centers for vertebral centra first become evident in the cranial thoracic region, after ossification of neural arches is well underway in all presacral regions (Fig. 1*C*). Centra then ossify in a caudal direction (Fig. 1 *D* and *E*). Ossification in the neck region begins cranially, and C7 is the last element to ossify its centrum, with the cervical centra delayed relative to the cranial thoracic centra. The lower neck region and sacrum are among the last elements to ossify (Fig. 1*D*), along with the sacrum (Fig. 1*E*). All 34 stages of dasypodids in our developmental series show the pectoral girdle elements (scapula and clavicle) adjacent to the cranial-most rib-bearing vertebrae.

Skeletogenesis in Three-Toed Sloths. As in other mammals, neural arches of the atlas and axis in *Bradypus* ossify first (Fig. 2*A*), followed by those in the caudal neck region (Fig. 2*B* and

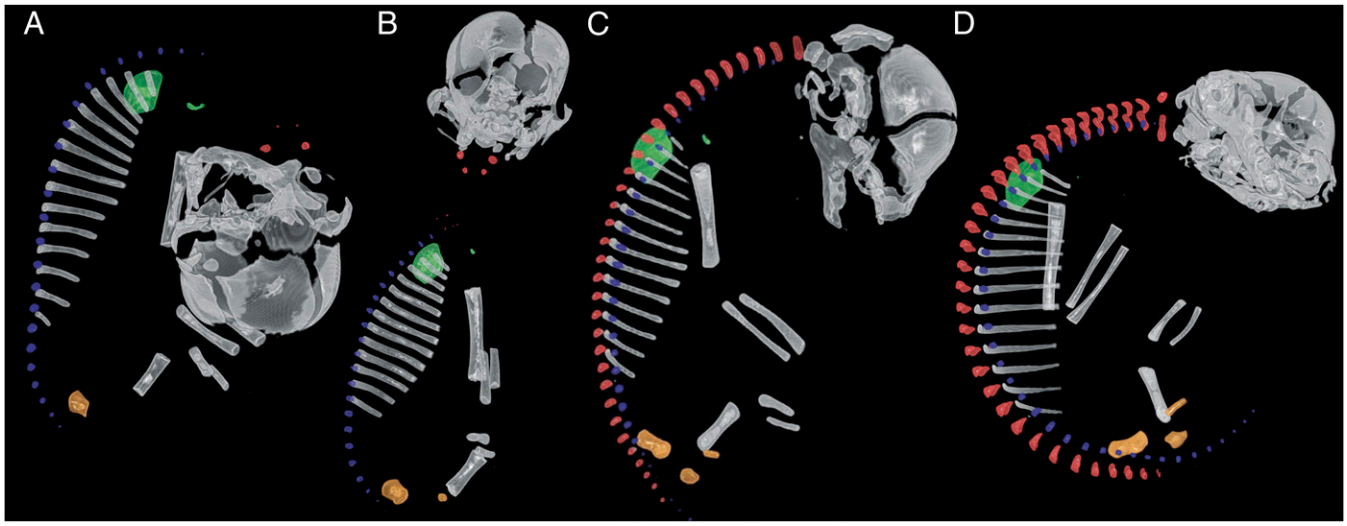

Fig. 2. Lateral view of 3D reconstruction of computerized tomography (CT) scans of skeleton in the three-toed sloth *Bradypus*: (*A*) *Bradypus variegatus* (ZMB 33812) CRL = 70 mm. (*B*) *Bradypus variegatus* (ZMB 41122) CRL = 80 mm. (*C*) *Bradypus tridactylus* (MNHN 1881-111) CRL = 100 mm. (*D*) *Bradypus tridactylus* (ZMB 18834) CRL = 120 mm. Vertebral neural arches are in red, vertebral centra are in blue, scapula and clavicle are in green, and ischium, ilium, and pubis are in orange. For clarity, right sides of the skeleton and elements of the autopod have been removed.

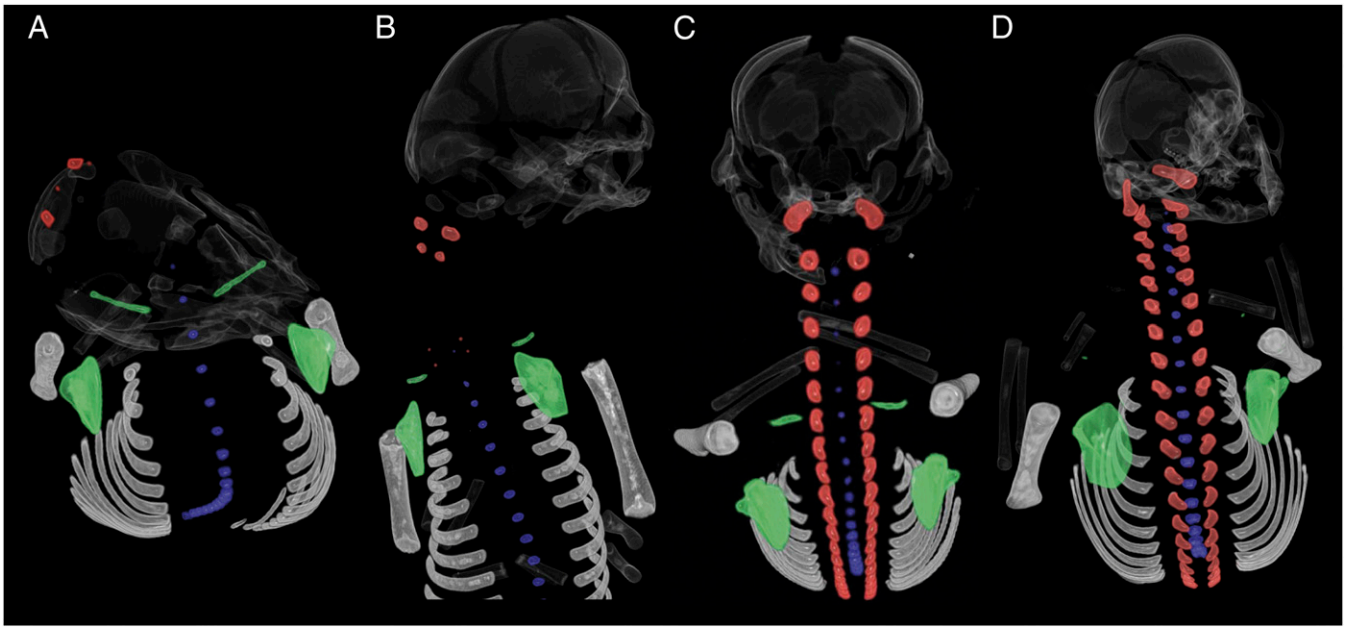

Fig. 3. Dorsal view of the neck in (*A*) *Bradypus variegatus* (ZMB 33812) CRL = 70 mm. (*B*) *Bradypus variegatus* (ZMB 41122) CRL = 80 mm. (*C*) *Bradypus tridactylus* (MNHN 1881-111) CRL = 100 mm. (*D*) *Bradypus tridactylus* (ZMB 18834) CRL = 120 mm. Vertebral neural arches are in red, vertebral centra are in blue, and scapula and clavicle are in green. For clarity, elements of the autopod have been removed.

Datasets S1, S2, S3, and S4). Ossification of neural arches then proceeds to the middle of the thoracic series, followed by those of the middle neck, with the distal sacral and caudal neural arches ossifying last (Fig. 2*C*).

However, unlike any other mammal in our sample (Fig. 1*A*), vertebral centra of *Bradypus* (Fig. 3*A*) begin ossification before all but the first two neural arches. Furthermore, ossification of the centra first appears among vertebrae of the lower neck, thoracic, and lumbar region (Fig. 2 *A* and *B*). The atlas is the last neck centrum to ossify, long preceded by that of the caudal-most ribless neck vertebra (Figs. 2*A* and 3*C*). Thus, the ossification spreads from the second neck vertebra in a caudal direction and from the last neck vertebra in a cranial direction to meet at the medial part of the series (Fig. 3*C*). The youngest specimens of our sample of *Bradypus* (Figs. 2 *A* and *B* and 3 *A* and *B*) are represented by *B. variegatus*. The ossification pattern of its caudal-most neck vertebrae resembles the cranial-most rib-bearing vertebrae of other mammals. That is, long-necked *Bradypus* shows ossification of its caudal neck centra simultaneously with ossification of its cranial rib-bearing vertebrae (Figs. 2*A* and 3*A*), not at the end of osteogenesis as in other mammals (Figs. 1 *C* and *D* and Fig. 4).

In *Bradypus*, the neck is weakly muscled, and the clavicle is absent in adults (15). However, we have observed rudimentary clavicles in all of our *Bradypus* specimens that do not yet show ossification of middle neck centra (Fig. 3). The clavicle is located above the cranial-most rib, adjacent to the ossified caudal-most neck centra (Figs. 2*A* and 3*A*). With the ossification of middle neck centra in older specimens, the clavicle disappears. Scapulae with at least two ossification centers are located near the first pair of ribs (Fig. 3).

In the pelvic girdle, the ilium ossifies first, followed by the pubis and ischium. A sacrum is not evident until well after central and neural arches elsewhere in the vertebral column are ossified. Lumbosacral and sacrocaudal transitions are correspondingly recognizable only at a relatively late developmental stage. However, we observed that the rostral part of the *Bradypus* ilium occupied a variable position across specimens, from the 28th (V28) to 30th vertebrae (V30).

Skeletogenesis in Two-Toed Sloths. All specimens of *Choloepus* correspond to relatively late stages, and thus, most vertebrae were ossified, including neck and upper thoracic centra (Dataset S4). Following Buchholtz and Stepien (13), *C. didactylus* typically has seven neck vertebrae, and *C. hoffmanni* has five or six neck vertebrae. In the primaxial skeleton, the distal sacral and caudal vertebrae are the last elements to start ossification. The small centra of the atlas suggests that it is the last presacral element to ossify, as in *Bradypus* (Datasets S1, S2, S3, and S4). In contrast to *Bradypus*, the neck is thickly muscled and the clavicle is well-developed in adult two-toed sloths (13). The clavicle occupies a forward position in front of neck vertebrae. The scapula is located adjacent to the boundary between rib-bearing and ribless vertebrae. The rostral part of the ilium again occupied a variable position, from V33 to V36.

Developmental Modularity of Neural Arches and Centra. Analysis of integration of developmental events using a rank correlation method (16) identified significant modularity between the neural arches and centra (Table S1). Comparisons of ossification sequences between *Bradypus* and individual mammal species, or composites thereof, showed that rank correlations are significantly greater within neural arches or within centra than in randomly generated alternative partitions or across all vertebral elements. For example, the comparison between *Bradypus* and a composite Boreoeutheria showed a nonsignificant correlation of 0.161 among all vertebral elements, a correlation of 0.528 ($P < 0.01$) among neural arches, and a correlation of 0.825 ($P < 0.01$) among centra. Centra were consistently more integrated than neural arches in all placental mammal comparisons.

Discussion

Axial Shift in Sloths. All mammals in our sample show a conserved pattern of ossification sequences that distinguishes thoracic from cervical vertebrae. Most conspicuously, centra of the cranial-most thoracic vertebrae ossify before those of the caudal-most cervical vertebrae in all mammals with seven ribless vertebrae in the neck. We, therefore, propose this difference in ossification timing as a developmental boundary between cervical and

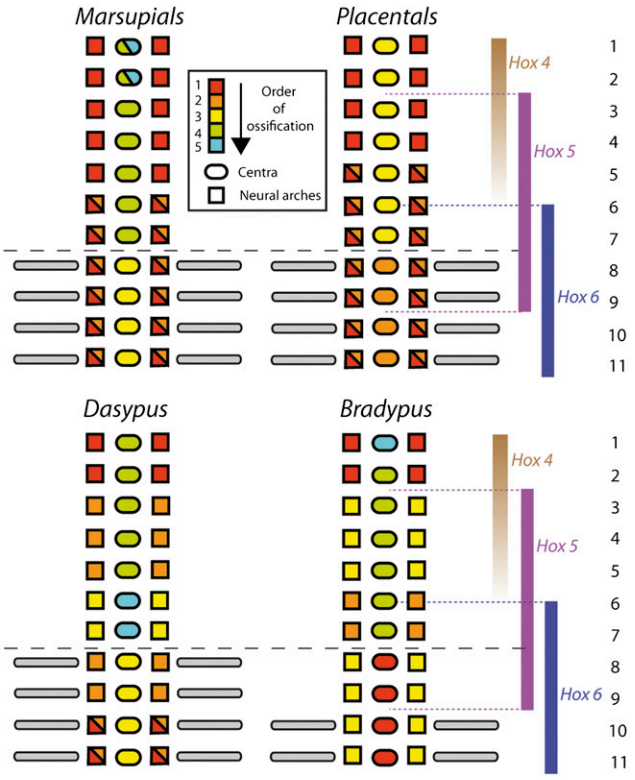

Fig. 4. Summary of ossification sequences in the first 11 mammalian vertebral elements. For each taxon, circles indicate centra, and squares indicate left and right neural arches. Colors represent the order of ossification. Hox expression boundaries in the mouse [redrawn from figure 5 in Wellik (25)] and vertebral segment identity are shown at right. Note the conserved timing of V7 centrum ossification across mammals, including sloths, and the overlap in *Hox5-6* expression in the V6–V9 region of the sloth neck.

thoracic vertebrae. Specimens of *Bradypus* with 8–10 neck vertebrae also show a difference in the timing of centra ossification, but unlike other mammals, the site of this difference does not correspond with the location of the first rib. Thus, the caudal-most neck vertebrae of sloths, traditionally considered to be cervical, exhibit developmental similarities with the most anterior thoracic vertebrae of other mammals (Fig. 4). The same pattern is observed in transgenic mice, which show an added cervical vertebrae with disrupted anatomy (figure 2a in ref. 17). We interpret these similarities in support of the PAS hypothesis that the neck of *Bradypus* is composed of seven cervical plus one to three ribless thoracic vertebrae.

Short-necked sloths (*C. hoffmanni*) possess five to six ribless neck vertebrae. Manatees are known to typically possess six ribless neck vertebrae (18). We predict that when data on their axial skeleton ossification sequences are available, they will show one to two cranial-most rib-bearing vertebrae that are developmentally cervical. That is, they will exhibit late ossification of their centra, after that of more distal, rib-bearing vertebrae and coincident with more proximal cervical vertebrae.

Homeotic Changes. Following previous authors (7, 19, 20), a homeotic transformation occurs when "one of the component parts of the axial skeleton assumes the morphological appearance and function of its neighbor either immediately preceding or immediately following it ... in distinction from meristic variations characterized by changes in total number of component parts" (p 407 in ref. 20). Therefore, intraspecific variation in sloths is homeotic when the overall vertebral number remains the same but the vertebral identities within that number change.

Buchholtz and Stepien (13) argued that vertebral variation in sloths does not qualify as homeotic, observing that the substantial variation in the number of neck vertebrae in sloths is strongly correlated with shifts in the position of the pelvis. Individuals with more neck vertebrae show a more distally positioned pelvis (figure 1 j–l in ref. 13). Using the definition above (20), a change in overall vertebral count (using the presacral count as a proxy) would qualify as meristic, not homeotic. However, studies on *Hox* transgenic mice, often referred to as homeotic mutants, have shown vertebral phenotypes similar to those seen in sloths, including correlation of the number of neck vertebrae and ribs with a displacement of the pelvis (17, 21–23). Hence, as defined in these studies, the term homeotic is still potentially applicable to both transgenic mice and sloths. Moreover, Buchholtz and Stepien (13) did not include vertebral counts in the caudal region of sloths (which are infrequently available in museum specimens) (24), leaving open the possibility that changes in presacral number were balanced in the postsacral region. Regardless of the strict definition of homeotic, we interpret our data as consistent with the PAS hypothesis of Buchholtz and Stepien (13). Importantly, patterning genes (e.g., *Hox*) influence phenotype differently in adult structures derived from primaxial vs. abaxial mesodermal sources (9). It is also interesting to note that the transition from neck to rib-bearing vertebrae in the three-toed sloth corresponds with the overlap in expression of *Hox5* and *Hox6*, as recognized in the mouse (Fig. 4) (25). Hence, changes in the morphology of this region are not caused by changes in *Hox* expression boundaries but could be related to differing contributions of primaxial vs. abaxial mesoderm during development. This emphasizes the importance of determining if and how mammals, such as sloths, may depart from the primaxial or abaxial boundary identified in the mouse (12), a possibility raised by Buchholtz and Stepien (13).

Sloth Vertebral Heterochrony. Although a simple craniocaudal sequence was first proposed for the ossification of the axial skeleton (26, 27), this sequence has subsequently proven to be more variable (26, 27). Bagnall et al. (28) showed that ossification centers of humans first appear in the cervical and lower thoracic/upper lumbar regions for the neural arches and the lower thoracic/upper lumbar regions for centra, corresponding to our observations in most other mammals. Our observations on a large sample of mammals confirm previous finds on humans (28), rodents (29–31), and bats (32) that the centra of the thoracic region ossify after neural arches, except in sloths.

In addition to showing developmentally thoracic vertebrae in the neck, sloths differ from other mammals in our dataset, including marsupials, in the late onset of neural arch ossification. To our knowledge, they are the only mammals to ossify vertebral centra before neural arches in the upper thoracic region. Our statistical analysis of modularity in neural arch and centra development further supports the idea that distinct developmental pathways contribute to axial skeleton regulation. Several studies have already identified different genetic influences on neural arch and centrum ossification (33–35). Koseki et al. (33) showed that *Pax-1* mutant mice are characterized by persistence of neural arches in the thoracolumbar region where centra are absent, a phenotype reminiscent of that reported in undulated strains of inbred mice (figure 4 in ref. 36). Moreover, the skeletal abnormalities in this mutant phenotype are mild in the cervicothoracic region (33). The fact that the cranial part of the vertebral column is less altered among transgenic mice is consistent with our observation of a conserved pattern of ossification sequence in the cervicothoracic region among all mammals studied. *Pax-1* expression was also observed in several other parts of the skeleton such as the ribs, sternum, shoulder girdle, and connection

between sacrum and pelvis (33, 35), showing that this gene is involved in patterning abaxial and primaxial derivatives.

The location of early ossifying centra in the caudal neck of *Bradypus*, contrasting with the ossification sequence observed in all other mammals, is consistent with the PAS hypothesis of Buchholtz and Stepien (13) and with their interpretation that the distal-most neck vertebrae in *Bradypus* are developmentally thoracic (as would be predicted if elements of the axial skeleton with distinct embryonic origins have shifted relative to one another during the course of mammalian evolution). Moreover, axial variation in sloths is not qualitatively distinct from that seen in studies of transgenic mice (17, 21, 22, 37), highlighting the common patterning mechanisms present in the skeleton throughout mammals.

Material and Methods

We sampled material from collections of the Museum für Naturkunde Berlin (ZMB), the Natural History Museum London (BMNH), the Museum National d'Histoire Naturelle in Paris (MNHN), the Museum of Zoology Cambridge (UMZC), the Australian Museum (AUM), South Australian Museum (SAM), the Macquarie University Marsupial Reproduction Laboratory (MUQ), and the Paleontological Institute and Museum of the University of Zürich (PIMUZ). A total of 20 unsexed sloth fetuses were examined, representing both extant genera (*Bradypus* and *Choloepus*) and four species: *B. tridactylus*, *B. variegatus*, *C. didactylus*, and *C. hoffmanni* (38, 39). Species identification was based on collection data and cranial anatomy (38) and was possible for 15 of our 20 specimens (Datasets S1, S2, S3, and S4). Assignment to a relative developmental stage was based on size and number of discrete ossification centers throughout the skeleton following information by Bagnall et al. (28).

We also studied 34 fetuses of three species of the cingulate xenarthran *Dasypus*: *D. novemcinctus*, *D. septemcinctus*, and *D. kappleri*. Species-level identification for some museum specimens was unavailable (Datasets S1, S2, S3, and S4). The analysis also included data for several groups as listed in Datasets S1, S2, S3, and S4: one monotreme (*Ornithorhynchus*), six marsupials (*Cercartetus*, *Dasyurus*, *Isoodon*, *Petaurus*, *Trichosurus*, and *Macropus*), and seven placentals (*Mogera*, *Cryptomys*, *Talpa*, *Condylura*, *Capra*, *Rhabdomys*, and *Loxodonta*). The results of the ossification sequences in xenarthrans were compared with published accounts of other placental mammals, including *Homo sapiens* (28), *Meriones unguiculatus* (29), *Mesocricetus auratus* (30), *Rattus norvegicus* (31), and *Myotis lucifugus* (32). Marsupial specimens were sourced from collections of the Australian and South Australian museums, as listed in Weisbecker et al. (40) (Datasets S1, S2, S3, and S4).

To test the hypothesis that neural arches and centra comprise two independent developmental modules in terms of ossification timing, we applied the rank correlation-based method by Poe (16), which compares the observed Kendall's τ from a comparison of two taxa against a distribution of Kendall's τs generated from random alternative partitions of the two sequences. Comparisons are made between pairs of taxa, usually either sister species or composite taxa, to represent nonterminal nodes, as described in detail by Poe (16), Goswami (41), and Goswami et al. (42). Kendall's τ was calculated separately for three sets: (*i*) neural arches and centra, (*ii*) neural arches only, and (*iii*) centra only; 1,000 alternative partitions were generated to test the significance of integration in the second and third sets. Comparisons were made between *Bradypus* and individual mammal genera (*Rhabdomys*, *Meriones*, *Cricetus*, *Mogera*, *Cryptotis*, *Dasyurus*, *Isoodon*, and *Cercatetus*) or *Bradypus* and composite taxa (Rodentia, Lipotyphla, and Boreoeutheria).

Skeletons were imaged using high-resolution tomography (μCT) at the University of Cambridge Department of Engineering, the Helmholtz Zentrum (Berlin), the Natural History Museum (London), and VISCOM SARL (Saint Ouen l'Aumône, France). The marsupial vertebral ossification data were obtained from projection images using a SkyScan 1172 Micro-CT scanner at the Electron Microscopy Unit of Sydney University or a SkyScan 1072 at the Adelaide Microscopy Unit at Adelaide University. Threshold values between ossified parts and soft tissues were substantial and easily allowed osteological reconstructions; 3D rendering and visualization were performed using Drishti v.1.0 (Drishti Paint and Render). All of the results obtained from 3D reconstructions were checked through the acquisition of shadow images, comparable with a conventional high-resolution X-ray as described in Weisbecker et al. (40). Ossification centers were readily apparent in both 3D reconstructions and shadow X-rays. Using different visualization techniques (clear staining and several CT scanners) to obtain ossification information does not represent a confounding issue, because differences in detection thresholds do not yield erroneous sequences (40).

ACKNOWLEDGMENTS. We are grateful to M. Herbin, C. Bens, F. Renoult, C. Denys, and J. Cuisin (Museum National d'Histoire Naturelle, Paris), Peter Giere and Frieder Mayer (Museum für Naturkunde, Berlin), Paula Jenkins and Roberto Portela Miguez (Natural History Museum, London), and their colleagues for access to comparative material. For access to material and facilities, we thank Frank Knight (University of Ozarks, AK), Richard Truman (Louisiana State University School of Veterinary Medicine, Baton Rouge, LA), the Laboratory of Paleontology, and the Institut des Sciences de l'Evolution de Montpellier. We thank Emily Buchholtz for her comments on the manuscript. A. Heaver (University of Cambridge), N. Karjilov (Helmholtz Zentrum Berlin), R. Abel (Natural History Museum), R. Lebrun (Institut des Sciences de l'Evolution de Montpellier), K. Lin (Harvard University), F. Landru, C. Morlier, G. Guillemain, and the staff from Viscom SARL (St. Ouen l'Aumône, France) provided generous help and advice with CT acquisition. We thank Mariella Superina for her help and advice in finding ontogenetical series of xenarthrans. We thank Boris Brasseur for providing living accommodation in Paris. We are also indebted to two anonymous reviewers and the editors for their contribution to improve the manuscript. We thank Mariella Superina for her help and advice in finding ontogenetical series of xenarthrans. We thank Boris Brasseur for providing living accommodation in Paris. We acknowledge financial support from Grant F/09 364/I from the Leverhulme Trust.

1. Bininda-Emonds ORP, Jeffrey JE, Richardson MK (2003) Is sequence heterochrony an important evolutionary mechanism in mammals? *J Mamm Evol* 10:335–361.
2. Galis F (1999) Why do almost all mammals have seven cervical vertebrae? Developmental constraints, Hox genes, and cancer. *J Exp Zool* 285:19–26.
3. Narita Y, Kuratani S (2005) Evolution of the vertebral formulae in mammals: A perspective on developmental constraints. *J Exp Zool B Mol Dev Evol* 304:91–106.
4. Sánchez-Villagra MR, Narita Y, Kuratani S (2007) Thoracolumbar vertebral number: The first skeletal synapomorphy for afrotherian mammals. *Syst Biodivers* 5:1–7.
5. Müller J, et al. (2010) Homeotic effects, somitogenesis and the evolution of vertebral numbers in recent and fossil amniotes. *Proc Natl Acad Sci USA* 107:2118–2123.
6. Murphy WJ, Pringle TH, Crider TA, Springer MS, Miller W (2007) Using genomic data to unravel the root of the placental mammal phylogeny. *Genome Res* 17:413–421.
7. Asher RJ, Bennett N, Lehmann T (2009) The new framework for understanding placental mammal evolution. *Bioessays* 31:853–864.
8. Buffon G, ed (1765) *Histoire Naturelle, Générale et Particulière, avec la Description du Cabinet du Roi* (Imprimerie Royale, Paris), Vol 13, pp 35–71.
9. Burke AC, Nelson CE, Morgan BA, Tabin C (1995) Hox genes and the evolution of vertebrate axial morphology. *Development* 121:333–346.
10. Wellik DM, Capecchi MR (2003) Hox10 and Hox11 genes are required to globally pattern the mammalian skeleton. *Science* 301:363–367.
11. Galis F, et al. (2006) Extreme selection in humans against homeotic transformations of cervical vertebrae. *Evolution* 60:2643–2654.
12. Burke AC, Nowicki JL (2003) A new view of patterning domains in the vertebrate mesoderm. *Dev Cell* 4:159–165.
13. Buchholtz EA, Stepien CC (2009) Anatomical transformation in mammals: Developmental origin of aberrant cervical anatomy in tree sloths. *Evol Dev* 11:69–79.
14. Frigo L, Wooley PA (1996) Development of the skeleton of the stripe-faced dunnart, *Sminthopsis macroura* (Marsupiala, Dasyuridae). *Aust J Zool* 44:155–164.
15. Miller RA (1935) Functional adaptations in forelimbs of sloths. *J Mammal* 16:38–51.
16. Poe S (2004) A test for patterns of modularity in sequences of developmental events. *Evolution* 58:1852–1855.
17. McIntyre DC, et al. (2007) Hox patterning of the vertebrate rib cage. *Development* 134:2981–2989.
18. Buchholtz EA, Booth AC, Webbink KE (2007) Vertebral anatomy in the Florida manatee, *Trichechus manatus latirostris*: A developmental and evolutionary analysis. *Anat Rec (Hoboken)* 290:624–637.
19. Bateson W (1894) *Material for the Study of Variation* (Johns Hopkins University Press, Baltimore).
20. Savin PS (1937) Preliminary studies of hereditary variation in the axial skeleton of the rabbit. *Anat Rec* 69:407–428.
21. van den Akker E, et al. (2002) *Cdx1* and *Cdx2* have overlapping functions in anteroposterior patterning and posterior axis elongation. *Development* 129:2181–2193.
22. Gaunt SJ, Drage D, Trubshaw RC (2008) Increased Cdx protein dose effects upon axial patterning in transgenic lines of mice. *Development* 135:2511–2520.
23. Akasaka T, et al. (1996) A role for *mel-18*, a Polycomb group-related vertebrate gene, during theanteroposterior specification of the axial skeleton. *Development* 122: 1513–1522.
24. Pilbeam D (2004) The anthropoid postcranial axial skeleton: Comments on development, variation, and evolution. *J Exp Zool B Mol Dev Evol* 302:241–267.
25. Wellik DM (2007) *Hox* patterning of the vertebrate axial skeleton. *Dev Dyn* 236: 2454–2463.
26. Mall FP (1906) On ossification centres in human embryos less than one hundred days old. *Am J Anat* 5:433–458.
27. Noback CR (1944) The developmental anatomy of the human osseous skeleton during the embryonic, fetal and circumnatal periods. *Anat Rec* 88:91–125.
28. Bagnall KM, Harris PF, Jones PRM (1977) A radiographic study of the human fetal spine. 2. The sequence of development of ossification centres in the vertebral column. *J Anat* 124:791–802.

29. Yukawa M, Hayashi N, Takagi K, Mochizuki K (1999) The normal development of Mongolian gerbil foetuses and, in particular, the timing and sequence of the appearance of ossification centres. *Anat Histol Embryol* 28:319–324.
30. Beyerlein L, Hillemann HH, Van Arsdel WC, 3rd (1951) Ossification and calcification from postnatal day eight to the adult condition in the golden hamster (*Cricetus auratus*). *Anat Rec* 111:49–65.
31. Strong RM (1925) The order, time, and rate of ossification of the albino rat (*Mus norvegicus albinus*) skeleton. *Am J Anat* 36:313–355.
32. Adams RA (1992) Stages of development and sequence of bone formation in the little brown bat, *Myotis lucifugus*. *J Mammal* 73:160–167.
33. Koseki H, et al. (1993) A role for Pax-1 as a mediator of notochordal signals during the dorsoventral specification of vertebrae. *Development* 119:649–660.
34. Wallin J, et al. (1994) The role of Pax-1 in axial skeleton development. *Development* 120:1109–1121.
35. Peters H, et al. (1999) Pax1 and Pax9 synergistically regulate vertebral column development. *Development* 126:5399–5408.
36. Grüneberg H (1950) Genetical studies on the skeleton of the mouse II. Undulated and its 'modifiers'. *J Genet* 50:142–173.
37. van den Akker E, et al. (2001) Axial skeletal patterning in mice lacking all paralogous group 8 Hox genes. *Development* 128:1911–1921.
38. Wetzel RM (1985) *Ecology of Armadillos, Sloths and Vermilinguas*, ed Montgomery GG (Smithsonian Institution Press, Washington, DC), pp 5–21.
39. Anderson RP, Handley COJ (2001) A new species of three-toed sloth (Mammalia: Xenarthra) from Panamà, with a review of the genus *Bradypus*. *Proc Biol Soc Wash* 114:114–133.
40. Weisbecker V, Goswami A, Wroe S, Sánchez-Villagra MR (2008) Ossification heterochrony in the therian postcranial skeleton and the marsupial-placental dichotomy. *Evolution* 62:2027–2041.
41. Goswami A (2007) Cranial modularity and sequence heterochrony in mammals. *Evol Dev* 9:290–298.
42. Goswami A, Weisbecker V, Sánchez-Villagra MR (2009) Developmental modularity and the marsupial-placental dichotomy. *J Exp Zool B Mol Dev Evol* 312B:186–195.